J Mol Model (2012) 18:4131–4139
DOI 10.1007/s00894-012-1414-3

ORIGINAL PAPER

Analyzing of expression of novel polypeptide complexes consisting of Shiga toxin B subunit and Adherence Fimbriae of *Escherichia coli* based on in silico modeling

Zeinab Noroozian · Mana Oloomi · Saeid Bouzari

Received: 7 December 2011 / Accepted: 26 March 2012 / Published online: 24 April 2012

Abstract Enterohemorrhagic (EHEC) and enteroaggregative (EAEC) are two pathotypes of diarrheagenic *Escherichia coli.* EAEC strains express adhesins called aggregate adherence fimbriae (AAFs) which the bacteria use to adhere to intestinal mucosa. EHEC virulence factor is Shiga toxin which belongs to the AB5 toxin family. B subunit, the nontoxic part of Shiga toxin (StxB), forms a homo pentamer and is responsible for binding to target cells. StxB has recently been proven to have adjuvant activity. In the current study we fused StxB encoding gene to 3' end of genes encoding two variants of AAFs, i.e., AAF/I and AAF/II. The in silico studies on tertiary structure and biochemical characteristics of Shiga toxin A subunit (StxA) revealed more resemblance to AAF/II than AAF/I. The constructs were prepared in a way that StxB could imitate its natural structure (pentamer formation) and its position (C-terminus) in the native toxin complex. The expression of these constructs showed the formation of AAF/II-B as a protein complex but with lower molecular mass than its expected size. In contrast, the AAF/I-B complex was not formed. Overall, the results of in silico studies and expression experiments together revealed that despite AAF/II-B expression, StxB failed to form pentamer. Therefore the observed protein complex has lower molecular mass. Since StxB is bound to AAF/II through disulfide bond, this bond prevents pentamer formation of StxB. However, due to the lack of disulfide bond between AAF/I and StxB, no protein complex is formed, thus StxB maintains its pentamer structure.

Z. Noroozian · M. Oloomi (✉) · S. Bouzari (✉)
Department of Molecular biology, Pasteur Institute of Iran,
Tehran, Iran 1316943551
e-mail: manaoloomi@yahoo.com
e-mail: saeidbouzari@yahoo.com

Keywords Aggregative adherence fimbriae · *Escherichia coli* · Protein complex · Shiga toxin B subunit

Introduction

Diarrheagenic *Escherichia coli* (*E.coli*) is the most common cause of diarrhea in children and adults [1]. Enterotoxigenic (ETEC), enteropathogenic (EPEC), enteroinvasive (EIEC), enterohemorrhagic (EHEC), diffusely adherent (DAEC) and enteroaggregative (EAEC) are the six clinically and pathogenically distinct pathotypes of diarrheagenic *E.coli* which have been recognized so far [2]. Endemic, epidemic and travelers' diarrhea are commonly due to EAEC pathotype [3].

EAEC is distinguished from other *E.coli* pathotypes by its ability to adhere to intestinal mucosa via formation of a biofilm on enterocytes. Aggregation happens through the formation of this biofilm which consists of many layers of bacteria covered with aggregative adherence fimbriae (AAFs) with a stacked-brick pattern. AAFs are extracellular matrix proteins related to Dr family of adhesins, which are encoded by a group of plasmids called pAA [1, 3]. AAF/I, AAF/II, AAF/III and Hda are four allelic variants of AAFs presented by different EAEC strains [4, 5].

The pAA plasmid carries a gene cluster which encodes a number of proteins associated with aggregative adherence phenotype. Only one gene is the structural gene of fimbriae (*aggA* for AAF/I and *aafA* for AAF/II) and others encode non-fimbrial adherence factors [6]. AAFs are the main factor used to colonize the bacteria on the mucosa, therefore they are appropriate candidates for vaccine studies [7].

Shiga toxin, also known as Stx, is the main virulence factor of EHEC pathotype. Stx is a member of AB5 toxin family. Toxins of this family contain a monomer catalytic domain called A subunit and a homo pentamer of a binding

fragment which is known as B subunit. Shiga toxin A subunit (StxA) performs RNA *N*-glycosidase activity on a specific site of eukaryotic ribosomes which disrupt the translation process [3, 8]. This 32 kilodalton (kDa) protein has a C-terminal α-helix tail (approximately 11A°) which locates above the surface [9]. Shiga toxin B subunit (StxB) plays a role in recognition and binding to surface receptors of target cells. Each 7.7 kDa B monomer is covalently linked with two other B molecules in order to form a central pore through which the projecting C-terminal tail of the StxA penetrates [8, 10] (Fig. 1). In *E. coli*, two tandem genes (*stxA*&*stxB*) encode Shiga toxin. These genes are separated only with a ribosomal binding site (RBS) consisting of nine base pairs [11]. Each gene is translated, folded and transported individually into the periplasm where the holotoxin is assembled [8]. Our previous studies demonstrated that vaccination of Balb/c mice with AAF/I and AAF/II could not induce immune response in the absence of any adjuvant [7]. Recently, the B subunit of *E.coli* Shiga toxin has been reported to be able to activate dendritic cells (DCs) and thus possess adjuvant activity [12]. It also has cytokine release activity and stimulates the induction of humoral immunoglobulinG (IgG) response [13, 14].

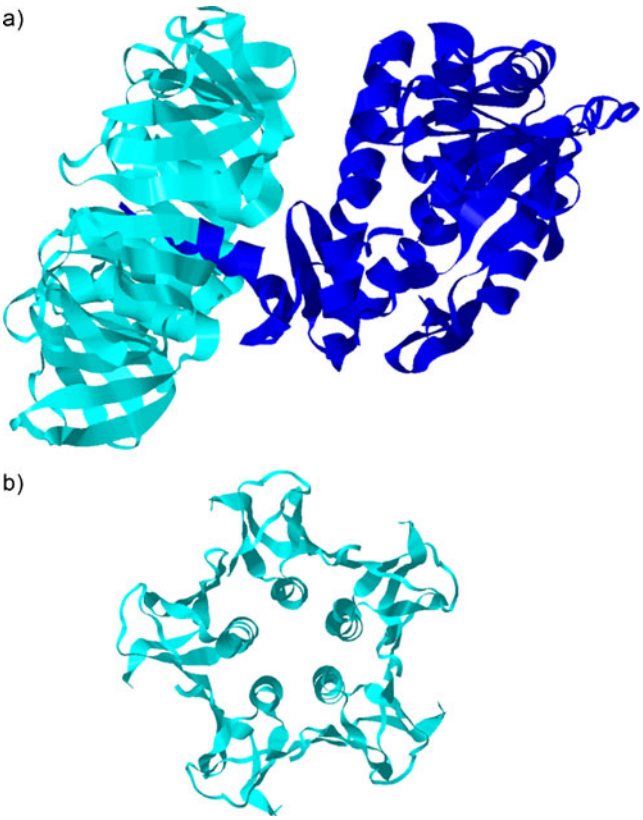

Fig. 1 Shiga toxin structure; (**a**) Tertiary structure of holotoxin; the protein in dark blue is the A subunit which enters to the pore of B subunit pentamer (in light blue) with non-polar α-helix C-terminal tail. (**b**) Pentamer structure of B subunit; each B monomer consists of two pairs of three stranded antiparallel β-sheets and one α-helix that lies above the surface. The α-helixes of 5 B molecules assemble together and form a doughnut-shaped structure with a central non-polar pore [8, 9]. Pdb file (PDB ID: 1R4Q) illustrated by 3D-Mol application of Vector NTI software

In the present communication, with the help of in silico studies we genetically fused the B subunit of Shiga toxin to C-terminus of AAF coding sequences mimicking the Shiga toxin structure. Hence, the conformation and expression of the constructs are discussed here.

Materials and methods

In silico analysis of proteins structures

Sequences of *stxA-stxB*, *aafA* and *aggA* fragments were obtained from NCBI database [15] with the following accession numbers respectively: (GenBank ID: AB015056), (GenBank ID: AF012835) and (GenBank ID: ECU12894). Tertiary structure of the Shiga toxin was obtained from the PDB database [16] of experimentally-determined structures of proteins (PDB ID: 1R4Q). ROBETTA [17] and QUARK [18] energy based protein structure prediction servers constructed the structures of AAF/I, AAF/II, B-AAF/I, B-AAF/II, AAF/I-B and AAF/II-B proteins. 3D Molecule Viewer tool of Invitrogen and Jmol software were used for analysis of the structures. TopMatch server [19] was used for alignment of protein structures. ProtScale tool [20] was used for assessment of physical and chemical characteristics of amino acids.

Amplification of *aggA*, *aafA* and *stxB* genes

Genomic DNA of *E. coli* strains 17–2, 042 and O157 was extracted by High Pure PCR Template Preparation Kit (Roche), and used as template for amplification of *aggA*, *aafA* and *stxB* genes respectively. The following primers were designed to amplify the genes such that overlap regions between *stxB* and *aggA* or *aafA* were added to 5′ end of the *stxB* and 3′ end of *aggA* and *aafA*:

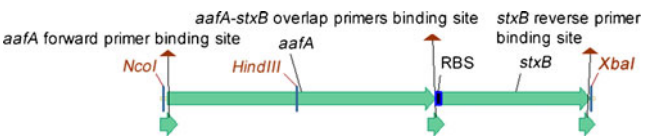

Fig. 2 *aafA-stxB* recombinant gene; The *aafA* gene is placed in the 5′ end of the recombinant gene. It ends with a TAA stop codon. RBS sequence fills the gap between two genes. The *stxB* gene starts right after RBS region. *NcoI* and *XbaI* restriction sites are placed at 5′ and 3′ ends of the recombinant gene respectively. Reverse primer of *aafA* and forward primer of *stxB* share mutual but complementary nucleotides consisting of 3′ end of *aafA*, RBS and 5′ end of *stxB*. Construction made by Vector NTI software

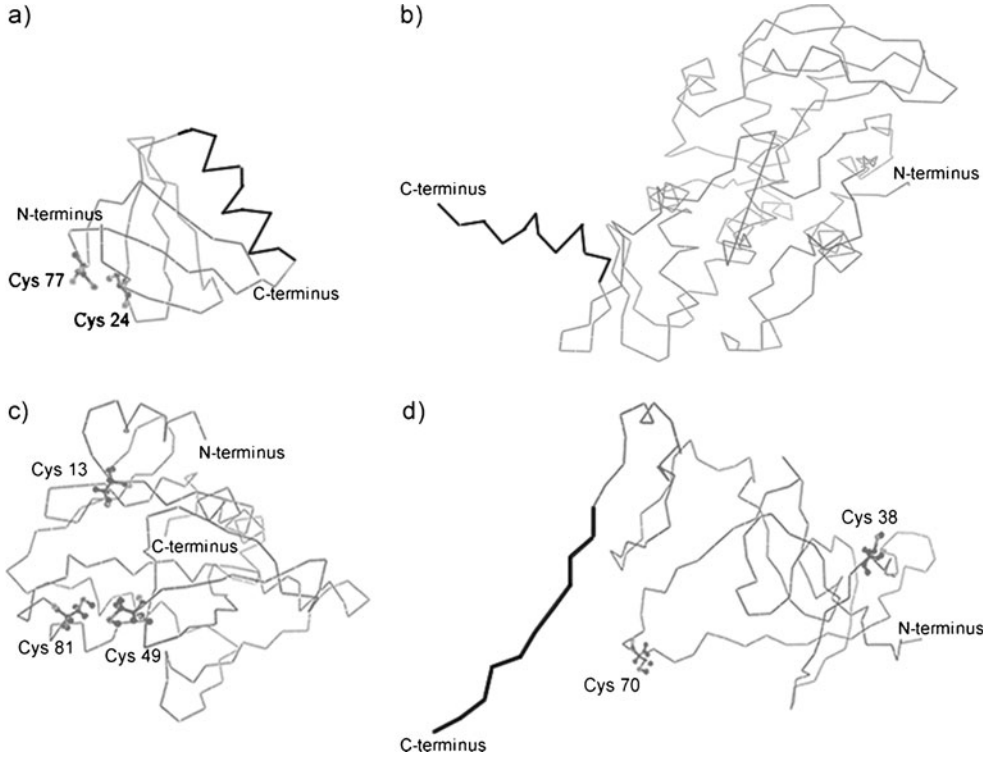

Fig. 3 Structural modeling of StxB, StxA, AAF/I and AAF/II proteins; (**a**) Tertiary structure of StxB monomer was obtained with homology modeling based on structure of StxB from *Shigella dysenteriae*. StxB monomer has one disulfide bond between Cys 24 and Cys 77 and one α-helix (shown in black) that lies above the surface of the molecule. (**b**) Tertiary structure of StxA was obtained with homology modeling based on the structure of StxA from *Shigella dysenteriae*. The C-terminal tail (shown in black) is responsible for binding to StxB pentamer. (**c**) Tertiary structure of AAF/I was obtained by ab initio modeling. It has three cysteine residues on positions 13, 49 and 81. Cysteine 49 forms a shared disulfide bond with cysteine 81 due to their proximity. Cysteine 13 has a free sulfur that is oriented toward interior region of the protein. This position prevents its binding to cysteine residues of other molecules. (**d**) Tertiary structure of AAF/II was obtained with ab initio modeling. It has a C-terminal tail (shown in black) and two cysteine residues on positions 38 and 70 which all are placed on the surface. Cysteine residues are ready for forming a disulfide bond with other molecules. Structures are illustrated with 3D-Mol application of Vector NTI software

Forward primer of *aggA*: 5'' CATGCCATGGCAAGGT GAAAATACATGAAA 3′; Reverse primer of *aggA*: 5′ TTTCATTTTACCCCCTTAAAAATTAATTCC 3′; Forward primer of *aafA*: 5′ CATGCCATGGCAATGAAA AAAATCAGAATG3′; Reverse primer of *aafA*: 5′ TTTCATTTTACCCCCTTAATTTGTCACAAG 3′; Forward primer of *stxB* for fusion with *aggA*:5′ GGA ATTAATTTTTAAGGGGGTAAAATGAAA 3′; Forward primer of *stxB* for fusion with *aafA*: ; 5′ CTTGTGA CAAATTAAGGGGGTAAAATGAAA 3′; Reverse primer of *stxB*: 5′ GCTCTAGACAACGAAAAATAAC TTCGCTG 3′.

The *Nco*I and *Xba*I restriction sites were included in forward and reverse primers respectively. The PCR

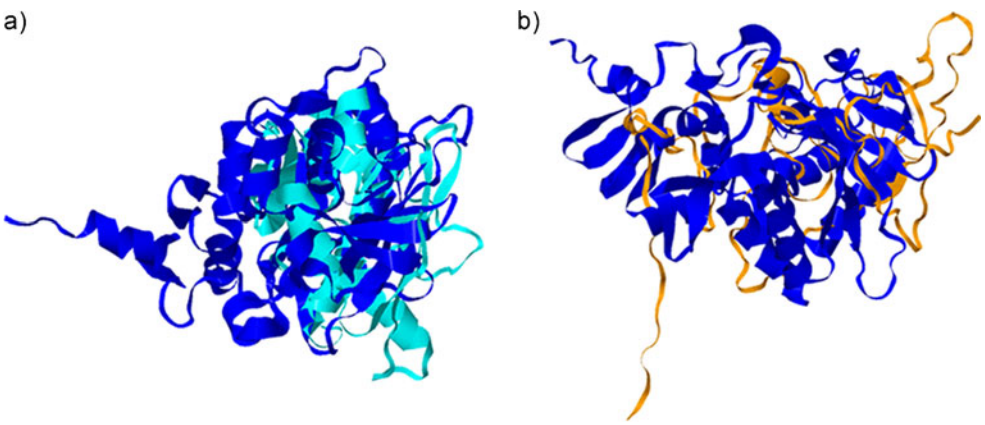

Fig. 4 Structural alignment of AAF/I and AAF/II with StxA; (**a**) AAF/I tertiary structure (in light blue) is aligned with StxA structure (in dark blue). (**b**) Alignment of predicted structures of AAF/II (in yellow) and StxA (in dark blue). Figure was captured from alignment results in TopMatch server [19] and prepared in Jmol tool

condition for amplification of the *aggA*, *aafA* and *stxB* consisted of a primary denaturation cycle of 94 °C for 5 minute (min), and 5 cycles of 94 °C for 1 min, 40 °C for 1 min and 72 °C for 1 min followed by 30 cycles of 94 °C for 1 min, 45 °C for 1 min and 72 °C for 1 min and a final extension time of 10 minute at 72 °C. The reaction mixture included 1 microliter (μl) Taq DNA polymerase (5 unit(U)/μl), 5 μl of 10X PCR Buffer, 1 μl $MgCl_2$, 5 μl Template DNA, 1 μl of each primer and 1 μl deoxynucleoside triphosphates (dNTPs) in a total volume of 50 μl. Finally, the PCR products were gel purified using gel extraction kit (CoreOne).

Production of *aggA-stxB* and *aafA-stxB* recombinant constructs

The eluted fragments were used as template for overlap PCR using forward primer of *aggA* or *aafA* and *stxB* reverse primer. The PCR condition included a primary denaturation time of 5 min at 94 °C followed by 10 cycles of 1 min at 94 °C, 1 min at 50 °C and 1 min at 72 °C, then 25 cycles of 1 min at 94 °C, 1 min at 50 °C, and 1 min at 72 °C and a final extension time of 10 min at 72 °C. The amplified fragments, AAF/I-B (822 bp) and AAF/II-B (781 bp), were gel purified, digested with *NcoI* and *XbaI* restriction endonucleases and cloned into the same digested ends of pBADgIII/A (Invitrogen) plasmid. To verify the cloning, the recombinant plasmids were subjected to DNA sequencing. The results showed 99 and 98 % similarity to the *aggA-stxB* and *aafA-stxB* sequences constructed on the basis of the sequences obtained from GenBank database (Fig. 2).

Expression of the AAF/I-B and AAF/II-B protein complexes

Top10 *E. coli* cells were transformed with the recombinant plasmids. For induction of the expression, the recombinant bacteria were cultivated in Luria Broth (LB) medium in the presence of 0.00002, 0.0002, 0.002, 0.02 and 0.2 % of L-arabinose for 4 hours. To evaluate the expression of the proteins by sodium dodecyl sulfate-polyacrylamide gel electrophoresis (SDS-PAGE), non-reducing loading buffer (free from any reducing agents such as Beta-mercaptoethanol (2ME) or dithiothreitol (DTT)) was used. For western blot analysis, proteins were electrotransferred to polyvinylidene fluoride (PVDF) nylon membrane (Roche). Detection of each recombinant protein was performed by using anti-B, anti-AAF (anti-AAF/I or anti-AAF/II) or horseradish peroxidase (HRP) conjugated anti-His antibodies. Other sets of SDS-PAGE were performed with samples prepared in reducing loading buffer for analyzing of expression of the AAF/II-B recombinant protein.

Table 1 Alignment parameters measured during protein structure alignment with TopMatch server [19, 23, 24]

Alignment	S [a]	c(q,t) [b]	c(t,q) [c]	Seq-Id [d]
AAF/I & StxA	38	22	13	0
AAF/II & StxA	154	96	53	18

[a] Number of residue pairs that are structurally equivalent - [b] Relative cover of the query (AAF/I or AAF/II) with respect to the target (StxA) expressed in percent – [c] Relative cover of target with respect to the query expressed in percent – [d] Percentage of sequence identity of query and target in the equivalent regions

Table 2 Estimated biochemical parameters of proteins with ProtScale tool [20]

Protein	pI [a]	Negative/ positive [b]	Half-life in *E. coli*	II[c]	Aliphatic index[d]	GRAVY[e]
StxA	9.63	25/31	>10 hours	33.10	94.03	0.083
AAF/I	10.02	9/21	>10 hours	12.87	89.53	−0.180
AAF/II	9.75	8/14	>10 hours	21.28	93.37	0.081

[a] Isoelectric point – [b] Number of negatively charged residues relative to positively charged amino acids - [c] Instability index - [d] Aliphatic index (relative volume of a protein occupied by aliphatic side chains) - [e] Grand average of hydropathicity

Tertiary structures of proteins

Protein structures were predicted by computer algorithms via two major models: comparative modeling which uses previously experimentally solved structures of homologous proteins [21] and *de novo* (ab initio) methods which predict structures that result in minimum global free energy for a protein amino acid sequence [22].

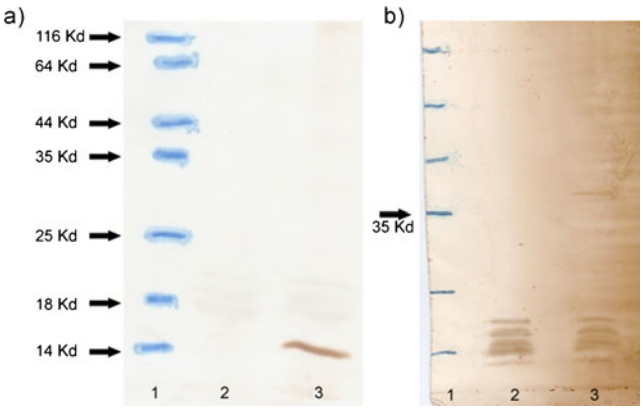

Fig. 5 Western blot analysis of AAF/I-B expression; (**a**) Detection of AAF/I-B protein complex with anti-AAF/I antibody. Lanes 1,2 and 3 respectively demonstrate protein molecular weight marker (MW), Top10 lysate containing pBAD vector lacking constructed recombinant gene (negative control), and Top10 lysate containing AAF/I-B expressed protein. (**b**) Detection of AAF/I-B protein complex with anti-B antibody. Negative control is shown by lane 2 and AAF/I-B expressed protein is shown by lane 3. (Elongation of incubation time lengths for improving attachment of anti-B antibody with B pentamer resulted in appearance of non-specific bands between 14 and 18 kDa in both lanes)

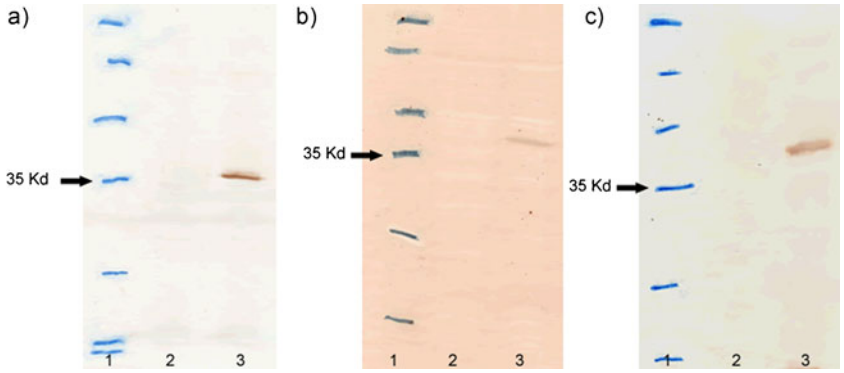

Fig. 6 Western blot analysis of AAF/II-B expression; (**a**) Expressed AAF/II-B protein complex in total lysate of the induced Top10 was detected with anti-AAF/II antibody (lane3). Lane 2 shows negative control. (**b**) Anti-B antibody revealed the protein complex at lane 3, and lane 2 indicates negative control. (**c**) Anti-His-HRP antibody detected the tag attached to StxB in lane 3. Lane 2 shows the negative control

The structures of the StxA and StxB were determined by the comparative modeling due to homology with StxA and StxB fragments from *Shigella dysenteriae*. These two toxins which originated from two different bacteria (i.e., *E.* coli and *S. dysenteriae)* have identical amino acid sequences and similar sizes with the homology level of 100 %.In contrast to commonly used proteins, limited reservoir of resolved protein structures are available in database for predicting the structure of most unknown or recombinant proteins. Therefore AAF/I and AAF/II tertiary structures were determined by ab initio modeling (Fig. 3).

Results

In silico analysis

AAF/I and AAF/II structures were separately aligned with StxA structure to find similarities (Fig. 4 a and b respectively). Table 1 shows the measured parameters which evaluate the similarity of structures of the two proteins with StxA. Figure 4 schematically demonstrates the covered regions of AAF/I and AAF/II structures with StxA.

Biochemical properties of amino acid sequences of AAF/I, AAF/II and StxA were measured and listed in Table 2. Isoelectric pH and aliphatic index corresponding to the thermostability of the proteins showed that no special treatment is required for expressing AAF/I and AAF/II instead of StxA. Negative amount of GRAVY for AAF/I demonstrated its hydrophilic attribute, and positive numbers in case of StxA and AAF/II showed their hydrophobic properties [25, 26].

Expression and detection of AAF/I-B protein complex

2ME reduces disulfide bonds and since each StxB monomer bears an internal disulfide bond which enhances the stability of its tertiary structure, therefore the bacterial lysate was prepared in the absence of 2ME. SDS-PAGE analysis of the protein complex revealed a band of about 35 kDa (data not shown). Surprisingly, western blot analysis using two different antibodies, anti-AAF/I(Fig. 5a) and anti-B (Fig. 5b),

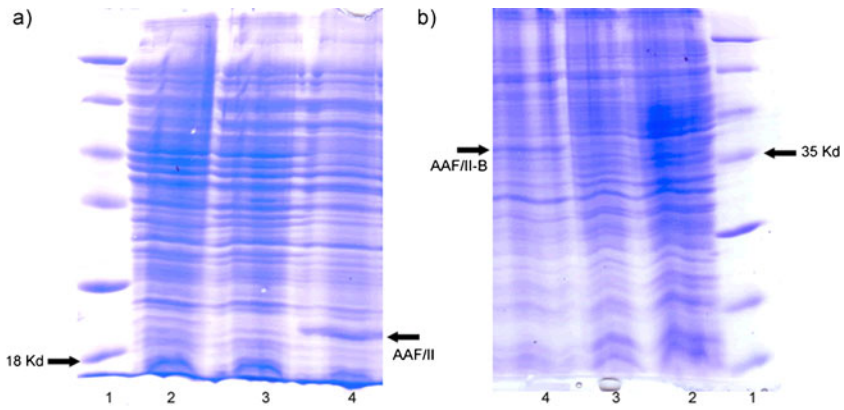

Fig. 7 SDS-PAGE analysis of AAF/II-B expression; (**a**) SDS-PAGE analysis of samples prepared in the presence of 2ME. Lane 1 is the molecular weight marker. Lanes 2 and 3 indicate negative control and lane 4 demonstrates expressed recombinant protein which shows a significant band of approximately 20 kDa, indicting the AAF/II alone. (**b**) SDS-PAGE analysis of samples prepared in the absence of 2ME. Lanes 2 and 3 indicate negative control and lane 4 shows a significant band of 35 kDa corresponding to the AAF/II-B protein complex

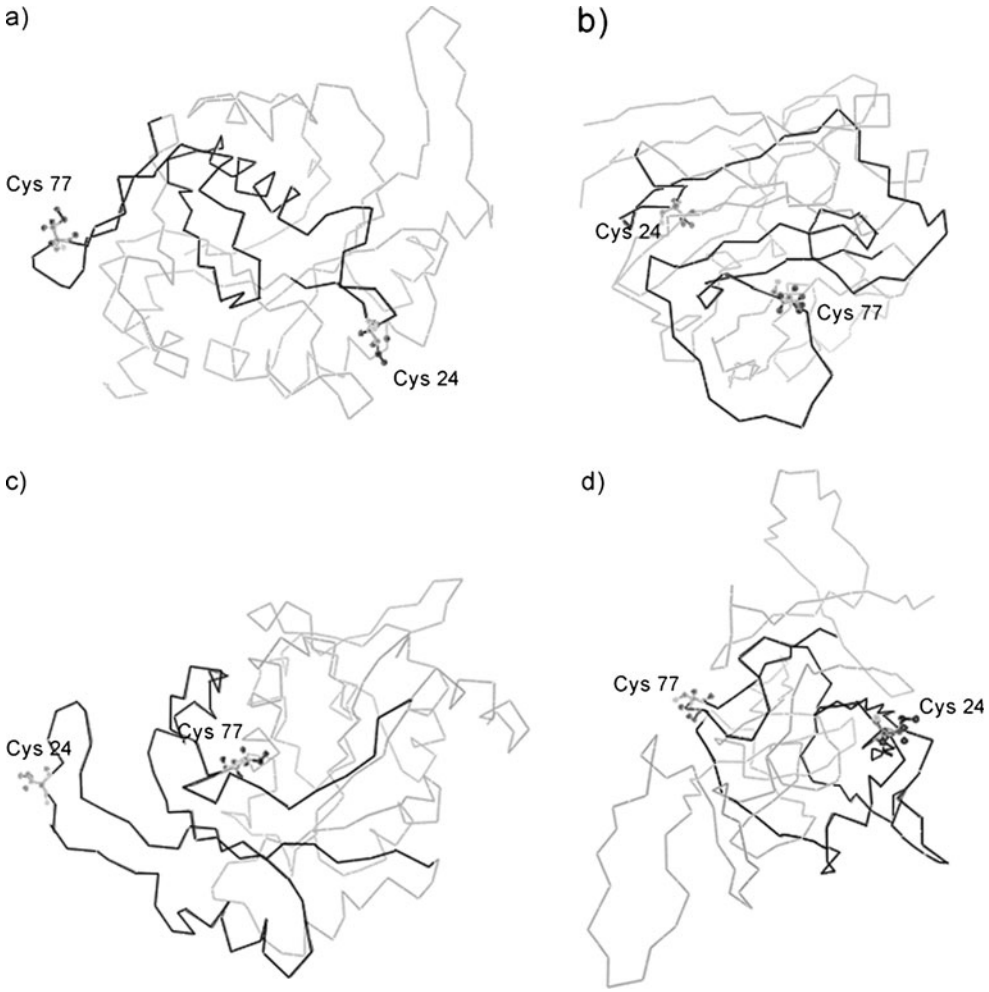

Fig. 8 Analysis of StxB structure attached to AAF/I or AAF/II (Cysteine residues of StxB are shown with side chains and residues of the StxB structure are highlighted with black lines in each picture); (**a**) In the structure of B-AAF/I (StxB placed at N-terminus), α-helix locates in the interior zone. (**b**) In B-AAF/II (StxB placed at N-terminus), α-helix is located in the surface but AAF/II molecule creates barrier and prevents one StxB from binding to other StxB monomers. (**c**) & (**d**) respectively demonstrate AAF/I-B and AAF/II-B both with C-terminal StxB. Secondary structure of the StxB in the C-terminus of each fusion protein is completely deformed. Pdb files of structures are illustrated with 3D-Mol application of Vector NTI software

revealed two separate bands, one with a molecular weight of 14 kDa corresponding to the AAF/I protein and a band of 35 kDa corresponding to the pentamer form of the StxB. It seems that AAF/I failed to form a complexwith B subunit and each protein is expressed separately.

Expression and detection of AAF/II-B protein complex

In contrast to AAF/I-B, the AAF/II-B expression and its consequent detection by western blotting using three different specific antibodies, anti-AAF/II (Fig. 6a), anti-B (Fig. 6b) and anti-His-HRP (Fig. 6c), revealed a single band of 35 kDa, indicating the formation of AAF/II-B protein complex.

Therefore it seemed that although AAF/II and StxB could form a protein complex, but its molecular weight is lower than the expected size which is approximately 50 kDa (17 kDa AAF/II+35 kDa StxB pentamer). Afterward, the SDS-PAGE analysis for AAF/II-B was repeated in the presence of the reducing agent 2ME. In this case a band of about 20 kDa (Fig. 7a) corresponding to the AAF/II alone was observed (Fig. 7).

Discussion

Recently, the B subunit of Shiga toxin has been reported to have cytokine release activity and has been injected with or fused to a partner protein [14]. It has been shown that Stx2B-Stx1B fusion protein stimulates the induction of humoral IgG response in mice [13]. Another experiment demonstrated that co-administration

Fig. 9 Possible states of disulfide bond(s) between AAF/II and StxB; (**a**) the schematic indicators of AAF/II, StxB and cysteine residues are defined. (**b**) Two disulfide bonds between one AAF/II and one StxB would make a complex protein with the size of 25.3 kDa. (**c**) Two disulfide bonds between one AAF/II and two StxB attached via a shared disulfide bond make a 33 kDa protein complex. (**d**) Three StxB molecules could bind to one AAF/II and create a protein complex with the size of 40.7 kDa. (**e**) A protein complex consisting of two AAF/II proteins and one StxB would have the size of 42.9 kDa. (**f**) A protein complex consisting of three (or more) AAF/II proteins and one StxB would form a 60.5 kDa (or larger) protein. (**g**) Two AAF/II and two StxB molecules create a 50.6 kDa protein. (**h**) Larger protein complexes consisting of three (or more) AAF/II and StxB molecules are less stable and less possible to be formed. Figure is created with Fireworks software ▶

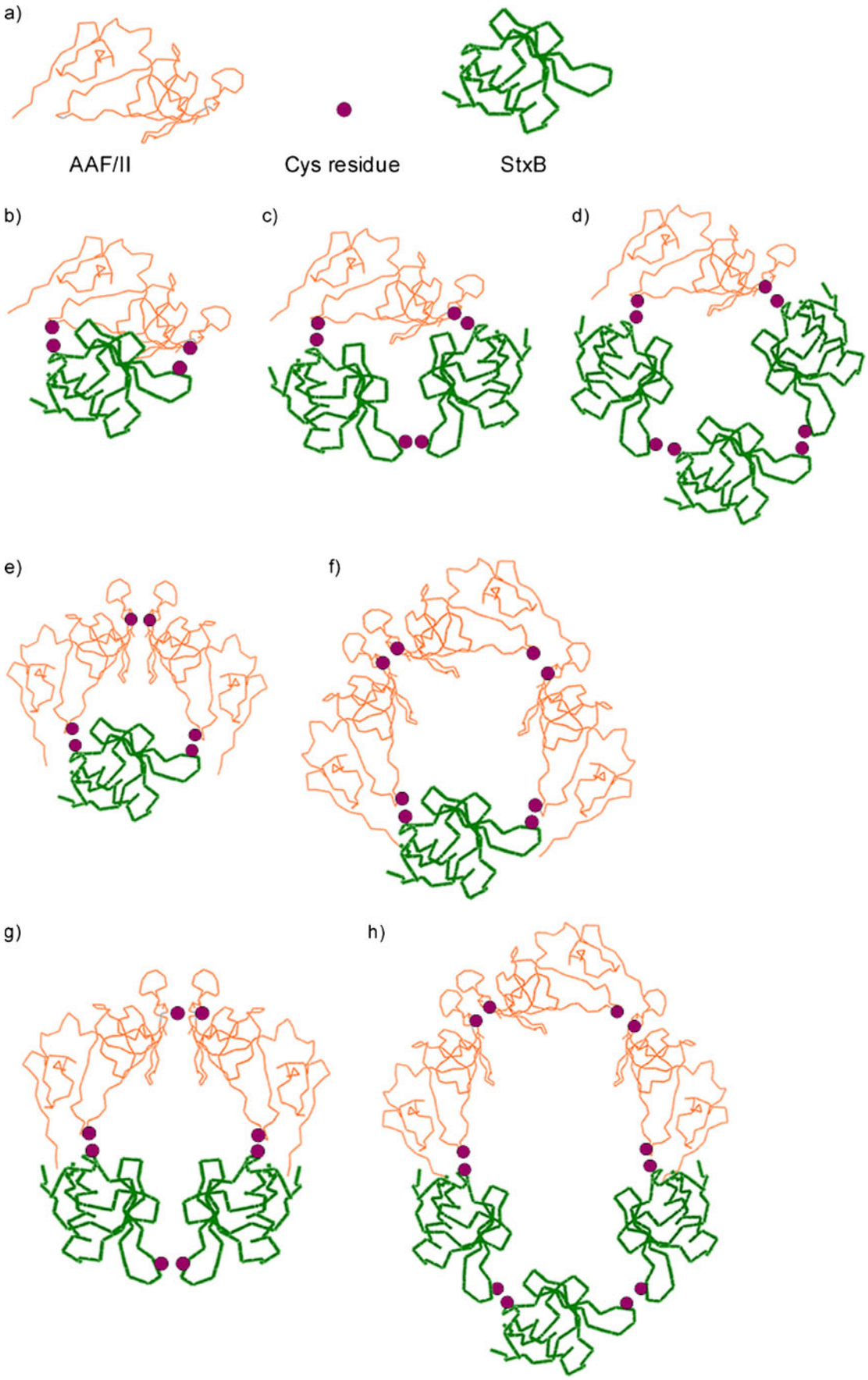
a)
AAF/II
Cys residue
StxB
b)
c)
d)
e)
f)
g)
h)

of StxB during immunization of mice with ovalbumin increased production of the antigen (Ag) specific IgG [12].

In our previous study, [27] fusion proteins containing AAF/I or AAF/II at their C-terminus and StxB at their N-terminus were constructed. However in the current study a novel strategy is used to fuse AAF/I and AAF/II to StxB. Positioning of the *aafA* or *aggA* genes (including their stop codon) at the 5′ end of the recombinant constructs followed by RBS preceding the *stxB* coding sequence resembles the native structure of the Shiga toxin genes. Hence, in the present study, designing of these protein complexes by in silico studies, and their expression and possibility of pentamer formation of B subunits as a complex partner were analyzed.

To study the possibility of pentamer formation we focused on two cysteine residues (Cys24 and Cys77) of StxB and disulfide bond formation. Each StxB monomer has two hydrogen bonds, three salt bridges and a disulfide bond between residues 24 and 77. These internal amino acid interactions form the secondary structure of the monomer which consists of two three-stranded antiparallel β-sheets and one α-helix (Fig. 3a). The α-helix is located on the surface of molecule and interacts with other α-helixes of StxB monomers which leads to the formation of pentamer structure [28].

When StxB is fused at the N-terminus or C-terminus of the AFF/I or AAF/II proteins without RBS in between, the structure of the StxB is shaped in a way that formation of disulfide bond is prevented. The α-helix which should be placed on the surface is located in the internal areas of the molecule or has spacial prevention from binding to other B monomers (Fig. 8).

Accordingly, we hypothesized that if we design the recombinant construct in a way that StxB could be translated separately as it occurs in the Shiga toxin, StxB monomers would fold naturally and form pentamer.

Due to this idea, AAF/I and AAF/II proteins were compared to StxA. Structural similarity of AAF/I or AAF/II with StxA is represented by Table 1. The similarity parameter S demonstrates that 154 residues of the AAF/II and StxA have equivalent structures. In contrast, the number of structural equivalent amino acids of AAF/I and StxA is only 38. Numbers of relative cover of each AAF/I or AAF/II with StxA, c (q, t), shows that more contents in StxA are covered with similar structures in AAF/II rather than AAF/I.

As represented by Table 2, also the AAF/II, rather than AAF/I, significantly resembles StxA in biochemical characteristics and expression conditions. The difference between amount of GRAVY of AAF/I and StxA, in addition to the close similarity of aliphatic indexes of AAF/II and StxA are keys to the above consequence.

Since a very special feature of AAF/II is that its C-terminal tail lies above the surface (Figs. 3d, 4b) which is very similar to C-terminal α-helix of the StxA (Figs. 3b, 4b), it could potentially penetrate to the central pore of B subunit pentamer as happens in the case of StxA. Hence, in contrast to the AAF/I-B, the AAF/II-B protein complex formation was observed in western blot analysis (Figs. 5–6).

Moreover, although AAF/II and Stx B could form a complex, a protein size of around 35 kDa which is lower than the expected size was obtained. Furthermore, SDS-PAGE analysis using reducing loading buffer containing 2ME showed that AAF/II and StxB are connected via disulfide bond instead of non-covalent bonds which attach StxA to StxB pentamer (Fig. 7). Therefore, although AAF/II and StxB complex formation occurred, StxB failed to form a pentamer, therefore, the protein band of around 35 kDa might be due to this configuration.

Considering this data, we analyzed the cysteine residues of StxB, AAF/I and AAF/II. Natural tertiary structure of StxB contains one disulfide bond between Cys24 located in third β-sheet and Cys77 located in sixth β-sheet (Fig. 3a). The role of disulfide bond is to stabilize the tertiary structure of StxB which prepares the platform (projecting α-helix) for pentamer formation. AAF/II has two cysteine residues at positions 38 and 70 which are laid on the surface and not involved in a mutual disulfide bond (Fig. 3d). Thus AAF/II has high affinity for binding to other proteins through s-s bond in the oxidized environment of periplasm.

The results of SDS-PAGE analysis for protein samples prepared in the presence of 2ME indicated that disulfide bonds are formed between AAF/II and B subunit. Therefore we assumed that due to this disulfide bond formation, the internal disulfide bond of StxB which is necessary for pentamer formation is not formed, and it is why a band with smaller size is obtained.

The two pairs of cysteine residues present in StxB and AAF/II are capable of creating a variety of disulfide bonds. The most probable forms are shown in Fig. 9. Formation of each variety produces a unique size of the protein complex which is calculated with the following formula:

$$(n)7.7\text{kDa} + (m)17.6\text{kDa} = \text{Protein complex size},$$

where n and m refer to the number(s) of StxB and AAF/II, respectively. 7.7 kDa is the size of StxB monomer and 17.6 kDa demonstrates the molecular weight of AAF/II.

In western blot and SDS-PAGE analysis of AAF/II-B protein complex the size of the obtained protein is approximately 35 kDa. Therefore, according to our proposed model (Fig. 9) the obtained protein complex consists of two StxB monomers attached to one AAF/II protein through disulfide bond.

Therefore the question arises why this is not the situation with AAF/I-B. The answer for this could be the situation of three cysteine residues in AAF/I (Fig. 3c), where a disulfide

bond between Cys 49 and Cys 81 is formed and its Cys13 is located in the interior region which is not accessible for disulfide bond formation with another protein. This situation makes AAF/I reluctant to form a disulfide bond with another protein, which provides the opportunity for StxB to form the pentamer structure shown in Fig. 5b. Corroboratively, Baibakov and colleges also expressed StxB pentamer with approximately the same condition and size [29].

Conclusions

In summary, for any protein complex to include pentamer B-subunit as its partner, two important points must be considered. First, in order to be able to attach to the StxB pentamer, the structure of the complex partner should be similar to StxA. Second, the condition should be so that the pentamer formation of B-subunit takes place without any hindrance.

Acknowledgments This project was financially supported by Pasteur Institute of Iran. We gratefully acknowledge the help of Dr. A. Jahanian-Najafabadi in preparation of the manuscript.

References

1. Flores J, Okhuysen PC (2008) Enteroaggregative *Escherichia coli* infection. Curr Opin Gastroenterol 25:8–11
2. Rúgeles LC, Bai J, Martínezetal AJ, Vanegas MC, Gómez-Duarte OG (2010) Molecular characterization of diarrheagenic *Escherichia coli* strains from stools samples and food products in Colombia. Int J Food Microbiol 138:282–286
3. Croxen MA, Finlay BB (2010) Molecular mechanisms of *Escherichia coli* pathogenicity. Nat Rev Microbiol 8:26–38
4. Harrington SM, Dudley EG, Nataro JP (2006) Pathogenesisofenteroaggregative*Escherichia coli*infection. FEMS Microbiol Lett 254:12–18
5. Boisen N, Struve C, Scheutz F, Krogfelt KA, Nataro JP (2008) New adhesin of enteroaggregative *Escherichia coli* related to the Afa/Dr/AAF family. Infect Immun 76:3281–3292
6. Elias WP Jr, Czeczulin JR, Henderson IR, Trabulsi LR, Nataro JP (1999) Organization of biogenesis genes for aggregative adherence fimbria II defines a virulence gene cluster in enteroaggregative *Escherichia coli*. J Bacteriol 181:1779–1785
7. Bouzari S, Dashti A, Jafari A, Oloomi M (2010) Immune response against adhesins of enteroaggregative *Escherichia coli* immunized by three different vaccination strategies (DNA/DNA, protein/protein, and DNA/protein) in mice. Comput Immunol Microbiol Infect Dis 33:215–225
8. Johannes L, Romer W (2010) Shiga toxins–from cell biology to biomedical applications. Nat Rev Microbiol 8:105–116
9. Jemal C, Haddad JE, Begum D, Jackson MP (1995) Analysis of Shiga toxin subunit association by using hybrid A polypeptides and site-specific mutagenesis. J Bacteriol 177:3128–3132
10. Fraser ME, Fujinaga M, Cherney MM, Melton-Celsa AR, Twiddy EM, O'Brien AD, James MN (2004) Structure of Shiga toxin type 2 (Stx2) from *Escherichia coli* O157:H7. J Biol Chem 279:27511–27517
11. Iwasa M, Makino S, Asakura H, Kobori H, Morimoto Y (1999) Detection of *Escherichia coli* O157:H7 from Musca domestica (Diptera: Muscidae) at a cattle farm in Japan. J Med Entomol 36:108–112
12. Ohmura M, Yamamoto M, Tomiyama-Miyaji C, Yuki Y, Takeda Y, Kiyono H (2005) Nontoxic Shiga toxin derivatives from *Escherichia coli* possess adjuvant activity for the augmentation of antigen-specific immune responses via dendritic cell activation. Infect Immun 73:4088–4097
13. Gao X, Cai K, Shi J, Liu H, Hou X, Tu W, Xiao L, Wang Q, Wang H (2009) Immunogenicity of a novel Stx2B-Stx1B fusion protein in a mice model of Enterohemorrhagic *Escherichia coli* O157:H7 infection. Vaccine 27:2070–2076
14. Adotevi O, Vingert B, Freyburger L, Shrikant P, Lone YC, Quintin-Colonna F, Haicheur N, Amessou M, Herbelin A, Langlade-Demoyen P, Fridman WH, Lemonnier F, Johannes L, Tartour E (2007) B subunit of Shiga toxin-based vaccines synergize with alpha-galactosylceramide to break tolerance against self antigen and elicit antiviral immunity. J Immunol 179:3371–3379
15. http://www.ncbi.nlm.nih.gov/gene. Accessed 14 March 2011
16. http://www.pdb.org. Accessed 12 April 2011
17. http://robetta.org. Accessed 8 June 2011
18. http://zhanglab.ccmb.med.umich.edu/QUARK. Accessed 13 June 2011
19. http://topmatch.services.came.sbg.ac.at. Accessed 14 June 2011
20. http://web.expasy.org/protscale. Accessed 21 April 2011
21. Jayaram B, Bhushan K, Shenoy SR, Narang P, Bose S, Agrawal P, Sahu D, Pandey V (2006) Bhageerath: an energy based web enabled computer software suite for limiting the search space of tertiary structures of small globular proteins. NucleicAcids Res 34:6195–6204
22. Bonneau R, Baker D (2001) Ab initio protein structure prediction: progress and prospects. Annu Rev Biophys Biomol Struct 30:173–189
23. Sippl MJ, Wiederstein M (2008) Anoteondifficultstructurealignmentproblems. Bioinformatics 24:426–427
24. Sippl MJ (2008) Ondistanceandsimilarityinfoldspace. Bioinforma 24:872–873
25. Ikai A (1980) Thermostability and aliphatic index of globular proteins. J Biochem 88:1895–1898
26. Kyte J, Doolittle RF (1982) A simple method for displaying the hydropathic character of a protein. J Mol Biol 157:105–132
27. Oloomi M, Bouzari S, Emami S (2009) A recombinant hybrid peptide composed of AAF adhesin of enteroaggregative *Escherichia coli* and Shiga toxin B subunit elicits protective immune response in mice. Eur J Clin Microbiol Infect Dis 28:1311–1316
28. Conrady DG, Flagler MJ, Friedmann DR, Vander Wielen BD, Kovall RA, Weiss AA, Herr AB (2010) Molecular basis of differential B-pentamer stability of Shiga toxins1 and 2. PLoS One 5:e15153
29. Baibakov B, Murtazina R, Elowsky C, Giardiello FM, Kovbasnjuk O (2010) Shiga toxin is transported into the nucleoli of intestinal epithelial cells via a carrier-dependent process. Toxins 2:1318–1335